Proc. Indian Acad. Sci. (*Chem. Sci.*), Vol. 115, Nos 5 & 6, October–December 2003, pp 401–410

Ultra thin films of nanocrystalline Ge studied by AFM and interference enhanced Raman scattering¶

S BALAJI[1], S MOHAN[1], D V S MUTHU[2] and A K SOOD[2,*]
[1]Department of Instrumentation, and [2]Department of Physics,
Indian Institute of Science, Bangalore 560 012, India
e-mail: asood@physics.iisc.ernet.in

Abstract. Initial growth stages of the ultra thin films of germanium (Ge) prepared by ion beam sputter deposition have been studied using atomic force microscope (AFM) and interference enhanced Raman scattering. The growth of the films follows Volmer–Weber growth mechanism. Analysis of the AFM images shows that Ostwald ripening of the grains occurs as the thickness of the film increases. Raman spectra of the Ge films reveal phonon confinement along the growth direction and show that the misfit strain is relieved for film thickness greater than 4 nm.

Keywords. Ion beam sputtering; ultra thin Ge films; interference enhanced Raman spectroscopy; phonon confinement; atomic force microscopy.

1. Introduction

There is a considerable interest in recent years to understand growth of germanium (Ge) films on silicon (Si) because of their usefulness in optoelectronic devices based on strained layer superlattices,[1] and strain-induced self-assembled quantum dots.[1] The latter have also been observed when Ge is grown on polymer surfaces, opening up the possibility of developing quantum lasers, single electron transistors and various other applications.[2] Stranski–Krastanov (SK) growth mode is the main mechanism which is observed in the growth of the Ge on Si. In this growth mode, a wetting layer is first formed up to a certain critical thickness (t_{cri}), which is strained because of the ~4% lattice mismatch between Ge and Si. After t_{cri}, the strain in the uniform two-dimensional layers is relaxed by the formation of three dimensional islands.[3] Depending on the surface orientation of Si and substrate temperature (T_s), the critical thickness and the shape of the islands are found to vary. The critical thickness is ~3–7 monolayers (ML) for Ge on Si(001)[4] whereas it increases up to 10 ML for (015) surface.[5] The 3D islands can be of different shapes like triangular on Si(111)[6], rectangular on Si(001) (at T_s = 700°C)[4] and hut clusters on Si(015).[5] Bimodal distribution of the islands were also observed for the Ge film prepared on Si(001) at a T_s of 600°C.[1] The strain in the initial layers of Ge have been measured by AFM force measurements on Si(111)[6] and on Si(100).[4] Waltz *et al*[6] have observed compressive stress ~6 GPa for Ge film of 0·8 nm thickness. TEM studies have also been performed to study the initial growth of Ge films on Si.[7]

In the initial growth of thin films, three types of growth can occur, depending on the surface free energy of the substrate (σ_s), surface free energy of the epilayer (σ_f) and the interface free energy (γ). If ($\sigma_f + \gamma$) > σ_s, the three dimensional island growth, called

¶Dedicated to Professor C N R Rao on his 70th birthday
*For correspondence

Volmer–Weber (VW) growth is favoured. If $(\sigma_f + g) < \sigma_s$, the layer by layer growth, called Frank van der Merwe growth can occur. If the film is strained due to lattice mismatch, the SK growth mode is preferred.[8] The growth of Ge on polymer substrate occurs via VW growth mode because of the non-wetting interface.[2] A similar growth mode is favoured for the formation of semiconductor films on insulator (SOI) because the surface free energy on insulators are considerably lower when compared with semiconductor substrates. SOI structures are gaining importance from the point of view of nano devices and single electron transistors.[9] In this context, initial growth stages of Ge ultra thin films on insulating ceria (CeO_2) surface are of considerable interest as the lattice constants of ceria are same as that of Si, giving a lattice mismatch of ~ 4%.

In this paper, single ion beam sputtered Ge films on ceria have been studied using AFM and interference enhanced Raman spectroscopy (IERS). As Raman spectroscopy is a powerful probe to estimate strain, crystallinity, and chemical nature of the materials, it is utilized to characterise the initial growth of Ge on ceria as well as to study confinement of phonons in the growth direction of the film.

2. Experimental details

Raman intensity from the ultra thin films can be enhanced by employing an optical interference technique called IERS.[10–14] This is basically an anti-reflection structure consisting of the following three layers: a bottom reflecting layer of aluminium, a middle transparent dielectric layer of ceria (CeO_2), and the top ultra thin layer of Ge which is to be investigated. The thickness of the ceria layer depends on the thickness of the Ge layer such that the reflection is minimum at the exciting laser wavelength. The calculations of the layer thicknesses have been done using the matrix method,[15] wherein optical constants of Ge and Al were taken to be the same as that of their bulk form and refractive index of CeO_2 layer is 2·3.

Aluminium films were prepared on Si substrates by thermal evaporation in a separate set-up. A hot cathode ion source of 3 cm diameter (Kaufman type) is used for sputter deposition of the films. CeO_2 film is prepared by the reactive ion beam sputtering with O_2 as the reactive gas. The Ar ions of energy 1 KeV with a beam current of 14 mA (7 mA) is employed to sputter the CeO_2 (Ge) target. The partial pressures of O_2 and Ar are $2{\cdot}0 \times 10^{-4}$ mbar and $1{\cdot}5 \times 10^{-4}$ mbar, respectively. Ceria films were prepared at a substrate temperature of 40°C and Ge films were prepared at substrate temperatures (T_s) of 40°C and 300°C. Raman spectra were recorded in the near backscattering geometry using DILOR XY spectrometer equipped with a CCD detector and 514·5 nm line of an argon ion laser as an excitation source (power of ~ 50 mW). AFM studies were done using the Digital Nanoscope-II in the contact mode. The nominal thicknesses of the films were initially estimated by the rate of deposition which is 4 nm/min for ceria and 3 nm/min for Ge film. Ultra thin layers of Ge of nominal thicknesses (1 to 10 nm) were deposited on CeO_2. The samples are named from A to E in the increasing order of nominal thickness: A (1 nm), B (2 nm), C (4 nm), D (7 nm) and E (10 nm).

3. Results and discussion

3.1 *Growth and morphology of Ge films*

Figure 1 shows the AFM measured surface features of germanium films A to E covering an area of 500×500 nm. The heights of the surface features are represented in gray

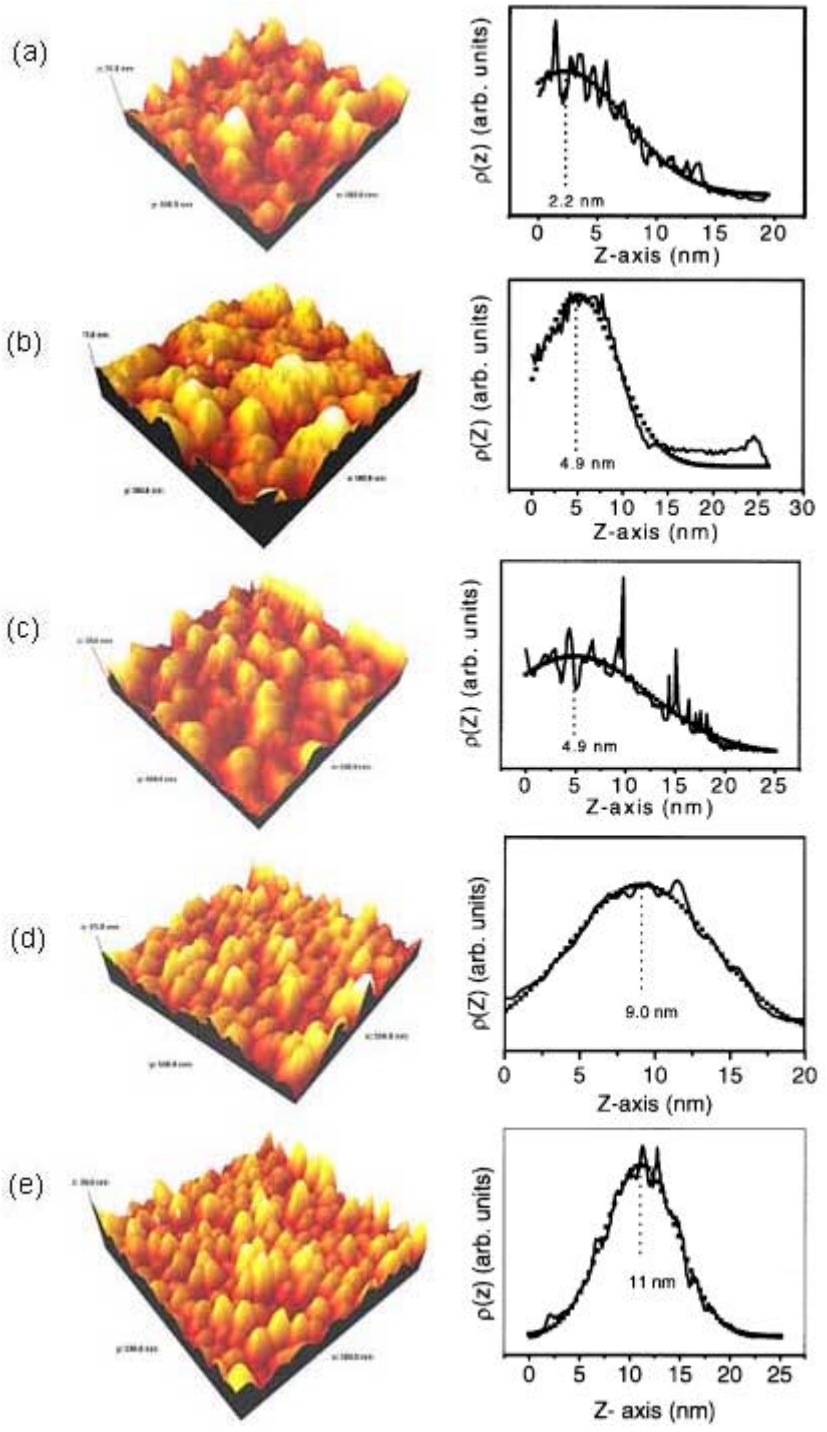

Figure 1. Surface morphology of the ultra thin Ge film samples A to E (left panels) and their corresponding height histograms (right panels). The dotted lines show the fitted Gaussian function.

scale of 256 gradation with the brighter pixel indicating the top of hillock and the dark pixel indicating the valley. Figure 1 also shows the histogram of the heights $r(Z)$ in nanometers. Figure 2 indicates the line profile $S(x)$ and the corresponding auto-covariance

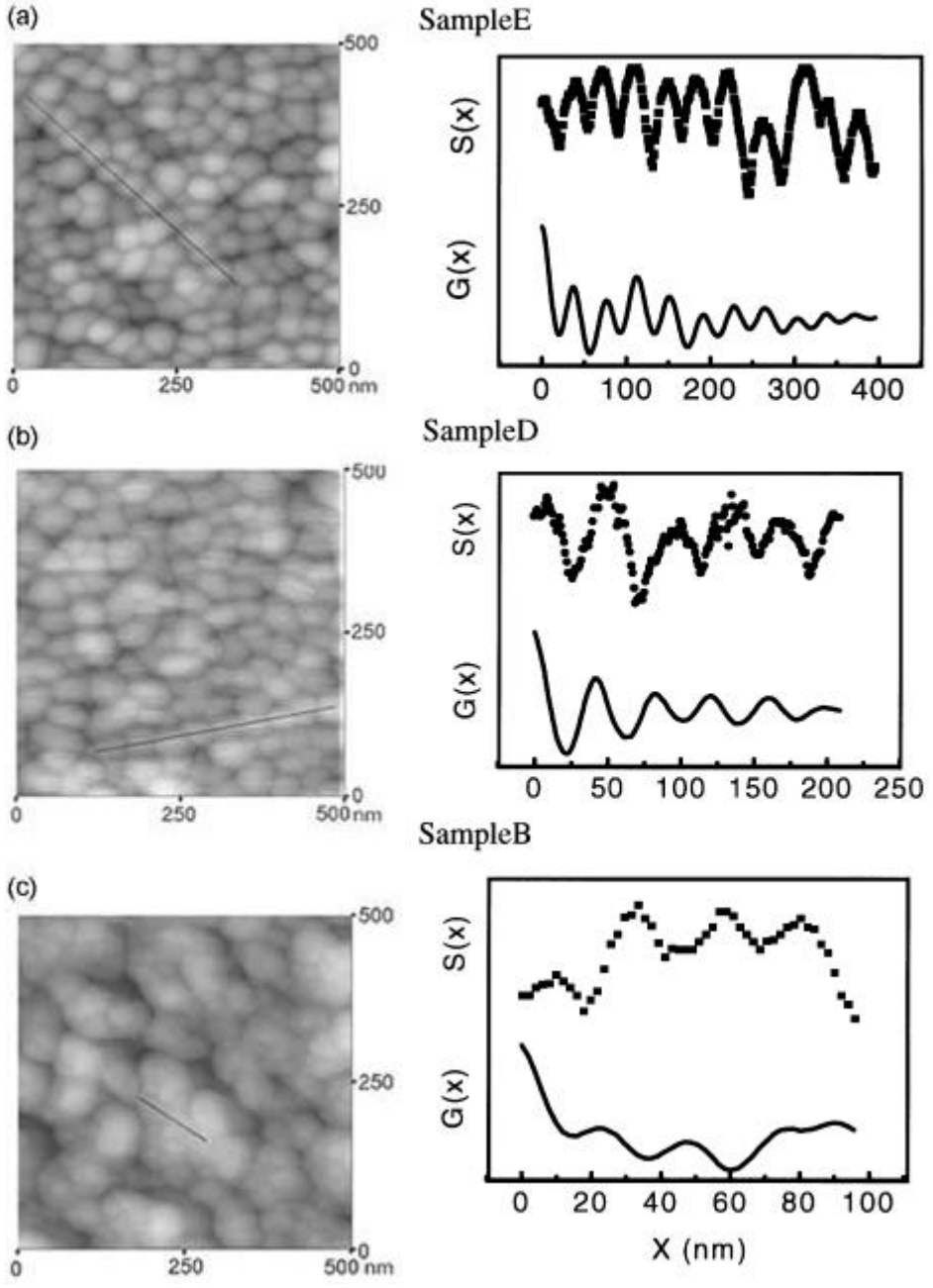

Figure 2. Left panels show two dimensional projections for the samples B, D and E. Right panels show the corresponding line profiles $S(x)$ and auto-covariance $G(x)$.

$G(x)$ for the samples B, D and E along the line marked in the AFM scans (left panel). The AFM image of the sample A in figure 1 shows a large number of voids along with some clusters of Ge crystallites, which is an indication of a discontinuous Ge film. The regions corresponding to the voids are discarded and the regions where the Ge crystallites are present are shown in the histogram plot of figure 1 for each sample. The first moment of the Gaussian distribution fitted to the measured histogram gives the average thickness of the Ge crystallites to be 2·2 nm for the sample A. The grain sizes obtained from the AFM images were found to be ~ 15–20 nm. Sample B also shows a presence of voids. Figure 1 shows the average height of the crystallites as 4·9 nm and the average grain size is ~ 20 nm (figure 2a). The small crystallites of Ge are observed across one single cluster. Sample C has more coverage of the Ge film with average thickness 4·9 nm. Surface features of sample D and E confirm the formation of continuous Ge film with average thicknesses of 9 and 11 nm, respectively and the average grain size is ~ 40 nm (figure 2b and c). From AFM studies, it is clear that during the initial growth of the film, cluster of 3D islands are formed. This is understandable because $(\sigma_f + \gamma_i) > \sigma_s$. The surface free energy[16] of Ge is 1·3 J/m^2 and 1·1 J/m^2 for ceria.[17] Further, in the ion beam sputter deposition process, the sputtered Ge atoms come and deposit with energies (~ 10 eV)[18] far greater than that of evaporation (~ 0·1 eV). This also contributes significantly to the growth of the films. These conditions favour the formation of 3D islands of Ge. This kind of growth mode, called Volmer–Webber growth mode, is also observed in the Ge films prepared on polymer substrates.[2] It can be seen from figure 2 that the grain size of the film increases as deposition time is increased. The increase in the grain size can be attributed to the Ostwald ripening of the grains.[1] The misfit strain gets relieved as the grains grow at the expense of the nearby smaller grains.

Figure 3 shows the structural changes (from amorphous to crystalline) in the Ge films of nominal thickness of 2 nm. Ge film grown at T_s of 40°C is amorphous as seen by a broad Raman mode centred at 270 cm^{-1} (figure 3a right panel).[14] The amorphous film has a cluster size of 60 nm as shown in figure 3a (centre panel). Ge film prepared at 300°C is crystalline as revealed by the sharp Raman mode at 301 cm^{-1} (figure 3b right panel). This film shows bigger clusters which are composed of smaller crystallites of size ~ 20 nm. This is inferred from the line profile $S(x)$ shown in figure 3b (centre panel).

3.2 *Analysis of the Raman spectra*

Figure 4 shows interference enhanced Raman spectra of the samples A to E. Raman spectrum of bulk Ge single crystal is also shown for comparison purposes. Raman signal for the sample A was weak and therefore, nine point averaging was done to smoothen the spectrum. Raman spectra of all the samples (except sample B) show a red shift in the peak position and an asymmetrical broadening on the lower frequency side when compared with the spectrum of the bulk Ge sample. The shift of the Raman band in thin films with respect to its value in bulk Ge can arise due to tensile or compressive strain and phonon confinement. We will first estimate the shift due to phonon confinement (PC).

Raman line-shape for low-dimensional systems is given by,[14,19–22]

$$I_c(\omega) \alpha \int_0^{q_{\max}} \frac{|c(q)^2}{[\omega - \omega(\vec{q})]^2 + \Gamma_0^2} d^3q, \tag{1}$$

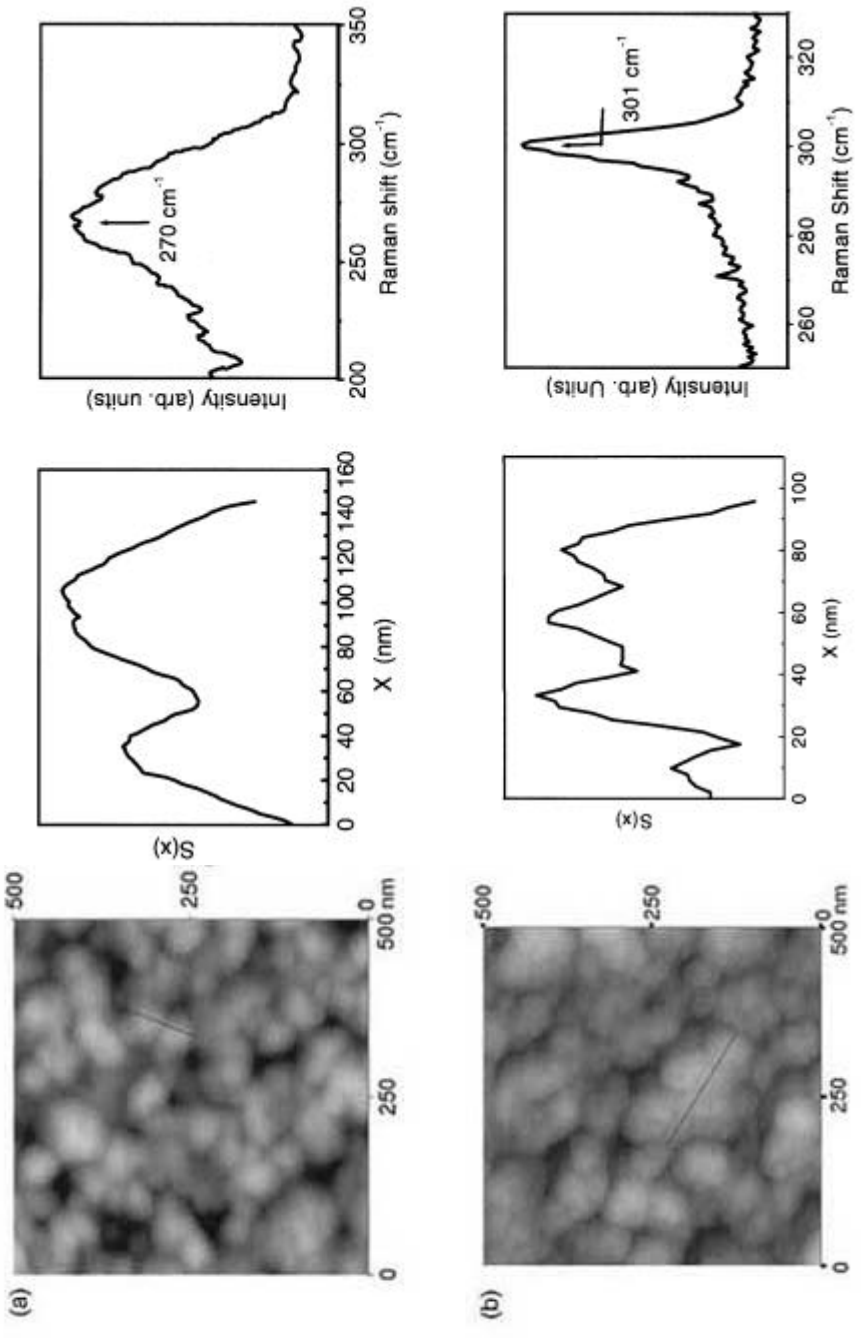

Figure 3. Two-dimensional projection of Ge films of nominal thickness 2 nm prepared at T_s = 40°C (**a**) and at T_s = 300°C (**b**). Their line profiles along the marked line in the left panels are shown in the centre panels. Raman spectra of the samples (right panels) show amorphous nature for (**a**) and crystalline nature for (**b**).

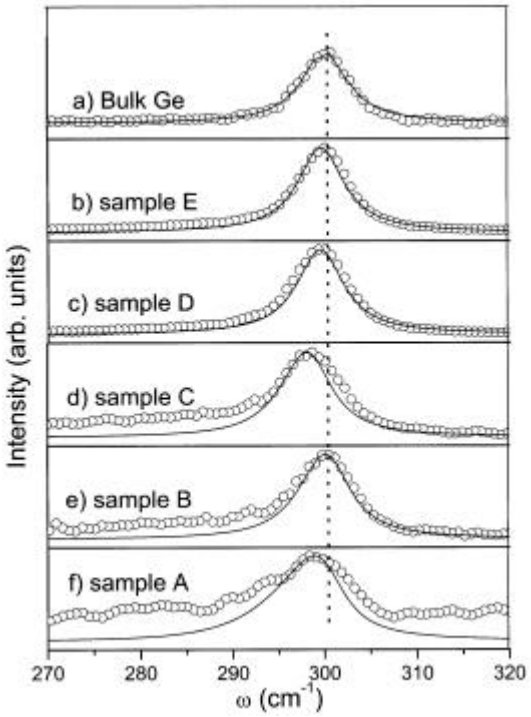

Figure 4. Shows observed Raman spectra (open circles) and the calculated spectra from the phonon confinement model (solid lines) for the samples A to E. Top panel shows the Raman spectrum of the bulk Ge. The calculated spectra for sample A and B are shifted up in the frequency to take into account the compressive strain, as explained in the text.

where $\omega(\vec{q})$ is the phonon dispersion curve of bulk Ge, Γ_o is the half width at half maximum (HWHM) of the Raman line of bulk Ge ($3{\cdot}0\,cm^{-1}$) and $c(q)$ is the Fourier transform of the phonon weighting function W(L). In many cases, the Gaussian form of the phonon weighting function W(L) has been used and the corresponding $c(q)$ is given as[14,22]

$$|C(q)|^2 = \frac{L}{\sqrt{32}} \cdot \frac{1}{8\pi^3} \cdot \exp\left(\frac{-q^2L^2}{16\pi^2}\right) \cdot \left|1 - erf\left(\frac{iqL}{\sqrt{32}\pi}\right)\right|^2 \quad (2)$$

The phonon dispersion $\omega(\vec{q})$ along (111) direction is taken from the inelastic neutron scattering measurement[23] and is same as used by us in ref. 12 and in ref. 14 (see inset in figure 5). Raman line shapes were calculated using (1) and (2) and the shift of the peak position $\Delta\omega(\Delta\omega = \omega_{film} - \omega_{bulk})$ and full width at half maximum 2Γ are extracted from the calculated spectra. Figure 5 (dashed lines) shows the calculated $\Delta\omega$ and 2Γ as a function of film thickness L. Also shown in figure 5 (star symbols) are the experimental values for the five samples wherein the value of L is used as measured by AFM. It can be seen that the observed line-width agree well with the calculated values for all the

samples, whereas the peak shifts agree only for samples C, D and E. The observed Raman peak positions for samples A and B are higher than the calculated values based on the phonon confinement model. We suggest that this due to the compressive strains because of the lattice mismatch between Ge and CeO_2. The lattice constant of CeO_2 (5·41 Å) is smaller by ~4% than that of Ge (5·65 Å), which would result in a blue shift of ~ 16 cm^{-1} of the Ge Raman line.[24] However, the discrepancy between the observed peak position and the PC model is much smaller than this value. This is because the misfit strain can partially relax in a discontinuous or polycrystalline Ge film grown on a polycrystalline CeO_2. For the layers of nominal thickness from 4 to 10 nm (sample C to E), the growth changes to 3D islands and in the process relaxes the strain, thereby Raman shift for the samples C, D and E agreeing with the PC model.

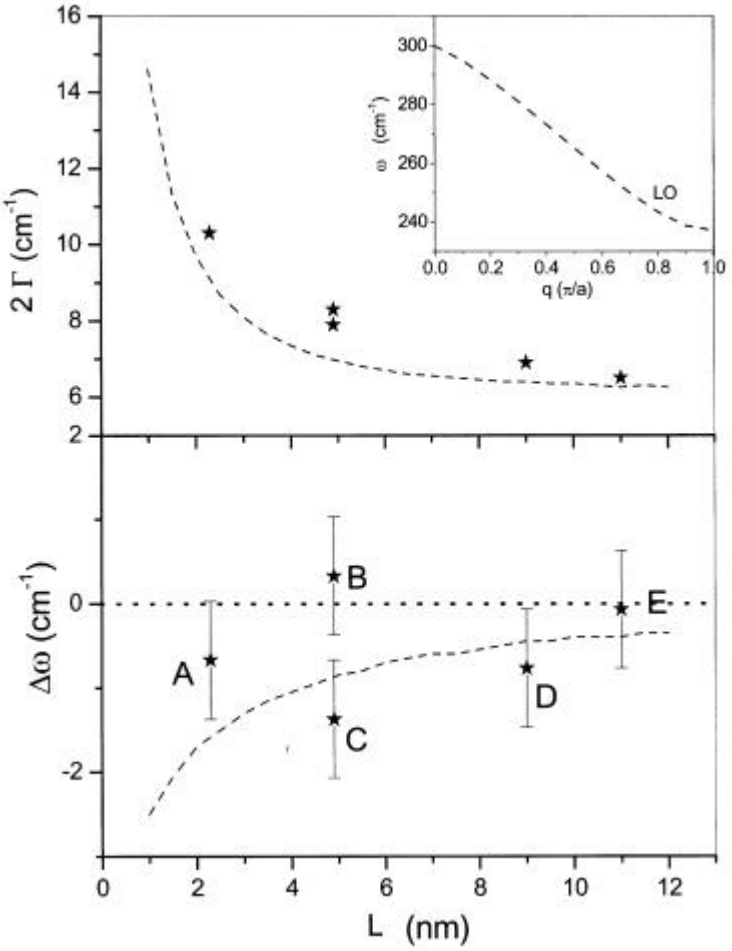

Figure 5. Shows the peak shift Δ*w* and line-width 2Γ as a function of film thickness. Star symbol shows the observed peak shift, the line-width and the calculated values using (1) and (2) are shown by the dotted lines (Inset (ref. 23) shows the phonon dispersion curve used in the calculation).

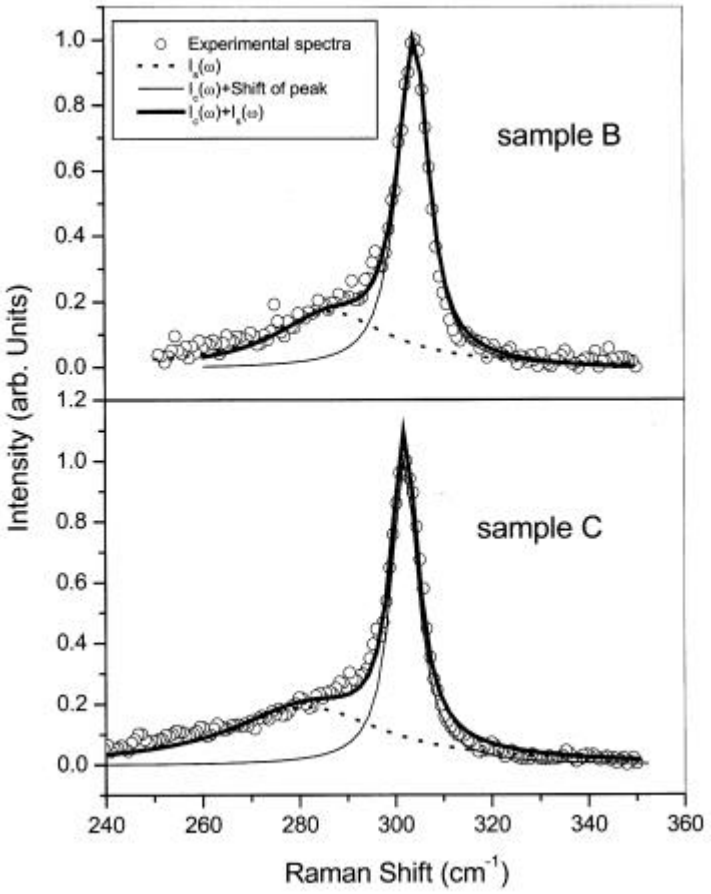

Figure 6. Raman spectra of samples B and C (open circles). The thick line is a resultant fit to $I_c(w)$ (1) (thin line) and a Lorentzian function (dotted line).

Figure 6 shows Raman spectra of the samples B and C. A shoulder at 280 cm^{-1} can be clearly observed on the lower frequency side of the main band. The observed spectra can be fitted (thick solid line) to a sum of $I_c(w)$ (1) and a Lorentzian centered at 280 cm^{-1} (dotted line). The component $I_c(w)$ has been shifted by + 1·2 cm^{-1} for sample B to take into account the compressive strain, as discussed above. The mode at 280 cm^{-1} is attributed to the surface phonon mode as discussed by Kanakaraju *et al.*[14] The essential source for the surface mode contribution arises from the surface to volume ratio of the Ge nano-crystallites. The grain sizes as well as the coverage increases for the samples D and E and hence the surface phonon is not prominent in their Raman spectra. We have not fitted the Raman spectra of sample A due to poor signal to noise ratio.

4. Conclusions

Ultra thin crystalline Ge films of nominal thicknesses 1 to 10 nm were deposited by ion beam sputtering technique. The growth and morphology of the Ge films were studied by

atomic force microscopy, which showed that the Ge films follow the Volmer–Weber growth mechanism. Ostwald ripening of the grains occur with an increase in the time of deposition. Raman spectra reveal that there is a compressive strain in samples A and B due to lattice mismatch between the Ge and ceria layers. Raman spectra also show a contribution from the surface phonon mode in samples B and C.

Acknowledgements

AKS thanks the Guest Editors for inviting him to contribute a paper to the special Festschrift Issue in honour of Prof. C N R Rao. We dedicate this paper to Prof. Rao on his 70th birthday and wish him many more years of exciting science and a healthy life. AKS and SM thank the Department of Science and Technology, Government of India, for financial assistance. We thank Dr Ganesan of Inter-University Consortium for DAE Facilities, Indore, for AFM measurements.

References

1. Gilberto Medeiros-Ribeiro, Bratkovski A M, Kamins T I, Ohlberg D A A and Williams S R 1998 *Science* **279** 353; Bean J C 1985 *Science* **230** 127
2. Das A K, Kamila J, Dev B N, Sundaravel B and Kuri G 2000 *Appl. Phys. Lett.* **77** 951
3. Mo Y W, Savage D E, Swartzentruber B S and Lagally M G 1990 *Phys. Rev. Lett.* **65** 1020
4. Wedler G, Walz J, Hesjedal T, Chilla E and Koch R 1998 *Phys. Rev. Lett.* **80** 2382
5. Tomitotori M, Watanadbe K, Kobayashi M K, Iwawaki F and Nishikawa O 1994 *Surface Sci.* **301** 214
6. Walz J, Greuer A, Wedler G, Hesjedal T, Chilla V and Koch R 1998 *Appl. Phys. Lett.* **73** 2579
7. Hammar M, LeGoues F K, Tersoff J, Reuter M C and Tromp R M 1996 *Surface Sci.* **349** 129
8. Ohring M 1992 *The material science of thin films* (California: Academic Press)
9. Celler G K and Sorin C 2003 *J. Appl. Phys.* **93** 4956
10. Connell G A N, Nemanich R J and Tsai C C 1980 *Appl. Phys. Lett.* **36** 31
11. Nemanich R J, Tsai C C and Connel G A N 1980 *Phys. Rev. Lett.* **44** 273
12. Kanakaraju S, Sood A K and Mohan S 1998 *J. Appl. Phys.* **84** 5756
13. Kanakaraju S, Sood A K and Mohan S 2000 *Phys. Rev.* **B61** 8334
14. Kanakaraju S, Sood A K and Mohan S 2001 *Curr. Sci.* **80** 1550
15. Heavens O S 1955 *Optical properties of thin solid films* (London: Butterworths Scientific Publications)
16. Stekolnikov A A, Furthmuller J and Bechstedt F 2002 *Phys. Rev.* **B65** 115318
17. Baudin M, Wojcik M and Hermansson K 2000 *Surface Sci.* **468** 51
18. Cuomo J J, Rosanagel S M and Kaufman H R (eds) 1989 *Hand book of ion beam processing technology* (New Jersey: Noyes Publication)
19. Tuinstra F and Koenig J L 1970 *J. Chem. Phys.* **53** 1126
20. Nemanich R J and Solin S A 1979 *Phys. Rev.* **B20** 329
21. Richter H, Wang Z P and Ley L 1981 *Solid State Commun.* **39** 625
22. Fauchet P M and Campbell I H 1988 *Crit. Rev. Solid State Mater. Sci.* **14** S 79
23. Nilsson G and Nelin G 1971 *Phys. Rev.* **B3** 364
24. Sutter P, Schwarz C, Muller E, Zelezny V, Gonacalves-Conto S and Von Kanel H 1994 *Appl. Phys. Lett.* **65** 2220